Proceedings of 9th IEEE International Conference
on CYBER Technology in Automation, Control, and Intelligent Systems
July 29- August 2, 2019, Suzhou, China

Modeling and Optimal Control of a Climb-Sliding Power Transmission Line Inspection Robot

Ahmad Bala Alhassan, Xiaodong Zhang, Haiming Shen and Jian Guo

Abstract— **This paper presents modeling and control of a sliding transmission line inspection robot modeled as mass spring damper system. The robot was proposed to inspect power lines using two arms attached to the overhead cables. The movement of the robot along the line as well as the disturbance due to gravitational force and wind are assumed to cause the power line to vibrate thereby causing the robot to be unstable. The mathematical model of the system was derived using Lagrange equations. Linear quadratic regulator (LQR) was designed for the optimal control of the induced vibrations. In addition, Pole placement control (PPC) was also designed and its performance was compared to the LQR. MATLAB simulations assessment of the robot behavior under initial condition, normal motion and external disturbances such as wind shows that LQR has better and efficient control as compared to the PPC.**

I. INTRODUCTION

Power transmission lines are used to carry high voltage power from generation stations to distribution stations for industrial and residential uses. Thus, the current modern society depends on the constant supply of the power for the day to day activities. However, failure to supply efficient and sufficient power could significantly affect the livelihood of any nation's security, transport system, health institutions among others. Thus, routine inspection is crucial for an early detection of faults along the power lines for reliable transmission of the high voltage power [1-3].

Traditionally, specialized workers inspect the power lines using a telescope from the ground or by climbing and moving along the overhead power lines. However, those techniques are unsafe, costly, time consuming and labor intensive. An alternative to the onerous manual inspection is the use the of transmission line inspection robots [4-5]. Many researchers have proposed those robots in order to replace the human in the loop manual inspection with autonomous robots. In addition, the robots are expected to identify and avoid any obstacle along the transmission lines. The most common type of obstacles associated with power lines are spacers, suspension clamps and aircraft warning balls [6].

Fascinatingly, over the last twenty years or so, there have been growing interests in the field of robotic particularly to automate the inspection of power lines. Some of the notable studies include; Expliner robot designed by Toyo power company [7-8], the Linescout robot designed by Canada hydro Quebec institute [9-10]. In addition, Shandong institute of science and technology proposed a three-arm power line inspection robot [11-12]. However, all of the aforementioned robots were large and heavy, which made them slow, consumes a lot of power and difficult to setup on the power lines. Moreover, due to complexity in deriving the mathematical equations of such robots, dynamic analyses of the robots are also very few. To provide a solution to those limitations, there is a need to provide light, portable and autonomous power line inspection robot as well as study its corresponding dynamic behavior.

In this study, vibration analysis and control of power inspection line is presented for safe, efficient and reliable inspection of power lines. The structure of the power line inspection robot is shown in Fig. 1. The dynamic model of the robot derived using Lagrange's equations was simulated in the MATLAB software. Linear quadratic regulator (LQR) as an optimal controller was designed for the control of the robot's induced vibrations. In addition, Pole placement control (PPC) was also designed and its performance was compared to the LQR.

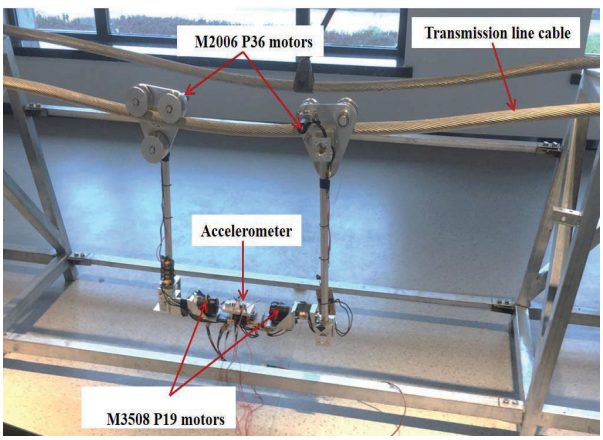

Fig. 1. The structure of the proposed robot.

*Research supported by the Science and technology innovation project of Shaanxi province, China (No.2018ZDXM-GY-093).

Ahmad Bala Alhassan is with the School of Mechanical Engineering, Shaanxi Key Laboratory of Intelligent Robot, Xi'an Jiaotong University, Xi'an, 710049, China (e-mail: amadkabo@stu.xjtu.edu.cn).

Xiaodong Zhang is with the School of Mechanical Engineering, Shaanxi Key Laboratory of Intelligent Robot, Xi'an Jiaotong University, Xi'an, 710049, China (phone: +8613355506818, e-mail: xdzhang@xjtu.edu.cn).

Haiming Shen is with the School of Mechanical Engineering, is with the School of Mechanical Engineering, Shaanxi Key Laboratory of Intelligent Robot, Xi'an Jiaotong University, Xi'an, 710049, China (e-mail: shenhaiming@stu.xjtu.edu.cn).

Jian Guo is with the School of Mechanical Engineering, Shaanxi Key Laboratory of Intelligent Robot, Xi'an Jiaotong University, Xi'an, 710049, China (e-mail: 1303263182@qq.com).

978-1-7281-0770-7/19/$31.00 © 2019 IEEE

Two types of vibrations were analyzed. These are: (i) free vibration which occurs due to the influence of the initial condition that represents the natural response of the system (ii) forced vibration which occurs due to an external excitation.

The paper is organized into 5 sections. Section II presented the description and dynamic model of the robot. Section III and IV presented the active control design and discussion of results respectively. Finally, section V presented the conclusion remark.

II. Description and Mathematical Model of the Power Transmission Line Inspection Robot

Based on the proposed structure of the power line inspection robot of Fig. 1, the robot basically has eight motors for its overall manipulations. Two of which are responsible for grasping the cables, two motors for motion along the transmission line, and four motors for robot rotations during obstacle avoidance.

At this point, this study focuses on sliding mode which uses the two rollers for sliding movement along the power line only. The derivation of the mathematical model of an inspection line robot is very complex due to its higher number of degrees of freedom and the associated nonlinearities. However, this study proposes a new method to model the robot in a mass-spring-damper configuration. The vertical components of the robots (gripper and arm) are considered to undergo axial stress when the robot moves along the power line. The designed schematic diagram of the robot is shown in Fig. 2, whereby y_1, y_2, (y_3, y_4, y_5) are the displacements of the rear arm of mass m_1, the front arm of mass m_2 and robot base of mass M respectively in the y-direction. F_w, F_1 and F_2, are the wind disturbance and actuator forces respectively. Also, γ_1 and γ_2 are the vertical input disturbances that correspond to sudden line sag, λ_1 and λ_2 are the distance between the midpoint of the robot to the right and left edges of the robot, respectively

In addition, c_1, k_1, and c_2, k_2 is the damping coefficient, stiffness of the rear and front gripper of the robot, respectively. c_3, k_3 and c_4, k_4 is the damping coefficient, stiffness of the rear and front circular arm of the robot, respectively. Finally, β is the angular displacement of the base of the robot and the moment of inertia, J for the rotation about the center of mass.

The Lagrange Equation given in [13] was used for deriving the mathematical equations of the robot as shown in Eq. (1).

$$\frac{d}{dt}\left(\frac{dT}{d\dot{q}_i}\right)-\frac{dT}{dq_i}+\frac{dU}{dq_i}=Q_i \quad ; \quad i=1,2,3\ldots n \tag{1}$$

where q_i is the independent generalized coordinate, Q_i is the total non-conservative generalized forces including external forces, frictional forces and damping forces, and T is the kinetic energy of the system and U is the potential energy consisting of energies due to gravity and elastic potential with *n* coordinate points given in Eq. (2).

$$T=\sum_{i=1}^{n}\frac{1}{2}m_i\dot{q}_i^2 \;;\; U=\sum_{i=1}^{n}\left(\frac{1}{2}k_iq_i^2\right) \tag{2}$$

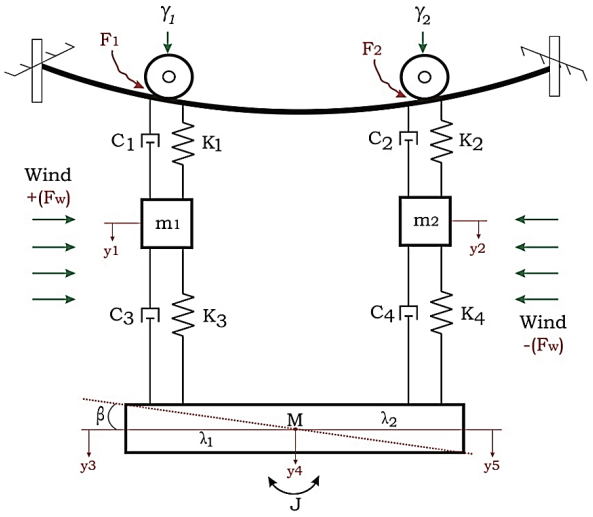

Fig. 2. Proposed schematic diagram of the robot.

Thus, the total kinetic and potential energies of the robot are given in Eqs. (3) and (4) respectively.

$$T=\frac{1}{2}\left(m_1\dot{y}_1^2+m_2\dot{y}_2^2+M\dot{y}_4^2+J\dot{\beta}^2\right) \tag{3}$$

$$U=\frac{1}{2}\left(k_1(y_1-\gamma_1)^2+k_2(y_2-\gamma_2)^2+k_3(y_3-y_1)^2\right)+\frac{1}{2}k_4(y_5-y_2)^2 \tag{4}$$

Solving for Eq. (1) using Eqs. (3) and (4) yields the second order dynamic equations for m_1, m_2, M and J as presented in [14]. It can further be seen that the forces F_1, F_2 and F_w acted horizontally while m_ig acted vertically. Thus, their equivalent resultants were utilized. The derived mathematical model can be represented in mass-spring damper form of Eq. (5).

$$m\ddot{x}+D\dot{x}+kx=f \tag{5}$$

where

$$m=\begin{bmatrix} m_1 & 0 & 0 & 0 \\ 0 & m_2 & 0 & 0 \\ 0 & 0 & M & 0 \\ 0 & 0 & 0 & J \end{bmatrix};$$

$$D=\begin{bmatrix} c_1+c_3 & 0 & -c_3 & \lambda_1c_3 \\ 0 & c_2+c_4 & -c_4 & \lambda_2c_4 \\ -c_3 & -c_4 & c_3+c_4 & -(\lambda_1c_3-\lambda_2c_4) \\ \lambda_1c_3 & -\lambda_2c_4 & -(\lambda_1c_3-\lambda_2c_4) & (\lambda_1^2c_3+\lambda_2^2c_4) \end{bmatrix};$$

$$k=\begin{bmatrix} k_1+k_3 & 0 & -k_3 & \lambda_1k_3 \\ 0 & k_2+k_4 & -k_4 & \lambda_2k_4 \\ -k_3 & -k_4 & k_3+k_4 & -(\lambda_1k_3-\lambda_2k_4) \\ \lambda_1k_3 & -\lambda_2k_4 & -(\lambda_1k_3-\lambda_2k_4) & (\lambda_1^2k_3+\lambda_2^2k_4) \end{bmatrix};$$

And $f = \begin{bmatrix} -k_1 r_1 - c_1 \dot{r}_1 + \sqrt{(m_1 g)^2 + (F_1 + F_w)^2} \\ -k_2 r_2 - c_2 \dot{r}_2 + \sqrt{(m_2 g)^2 + (F_2 + F_w)^2} \\ \sqrt{(Mg)^2 + (F_1 + F_1 + F_w)^2} \\ -\lambda_1 F_1 + \lambda_2 F_2 \end{bmatrix}$

III. Control Design

This section presents the linear quadratic regulator (LQR) and the pole placement control for stabilization of the robot. Consider the general state space model representation of any system described in Eq. (6) which can be obtained from the derived model in Eq. (5).

$$\dot{x} = Ax + Bu \quad ; \quad y = Cx \tag{6}$$

where x is the state vector, A is the constant system matrix, B is the constant input matrix, C is the output matrix.

The first step for any feedback control design is to check whether the states of the system are completely controllable or not. The controllability matrix M_C is given in Eq. (7) in [15].

$$M_C = \begin{bmatrix} B & AB & \dots & A^{n-1}B \end{bmatrix} \tag{7}$$

where n is the order of the system, here eight. The determinant of the matrix, M_C must be nonzero for a full state controllable system. For this system, using Eq. (5), $|M_C| \neq 0$ and hence, it is controllable. Thus, the controller can be directly design for this system. In this study, two states; the robot base position (y_4) and the angular displacement (β) of the robot are considered to be the concerned outputs to be controlled. These two outputs can completely describe the behavior of the system subjected to input signal. The state equations can be describe using the block diagram of Fig. 3 with reference signal *re* and *K* as the feedback control. The control signal u can be defined as in Eq. (8).

$$u = re - Kx \tag{8}$$

The main function of this controller is to track the reference input u to follow the desired output response and maintain the angular vibration, beta at zero thereby controlling the forced vibration. In addition, the control can archive those objectives by shifting the original Eigen values of the system to the desired location.

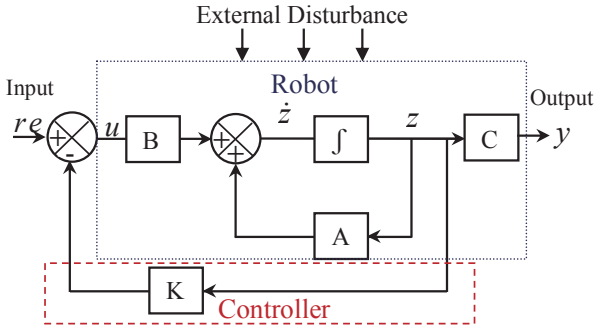

Fig. 3. Feedback control block diagram.

However, assigning the Eigen values depends on the required performance. These include the rise time, settling time, overshoot, among others. Its essential to always specify the control performance requirements of the control, in this study, the control objectives are constraints are: (i) maximum vibration overshot (O_p) of 10% (ii) settling time of 2 seconds (t_s) and (iii) zero steady state error.

A. Linear Quadratic Regulator (LQR)

LQR control is a powerful technique used in control design for complex systems with particular requirements where an optimal control that minimizes a given performance index (J) given in Eq. (9) is needed [16].

$$J = \int_0^\infty \left(x(t)^T Q(t) + u(t)^T Ru(t) \right) dt \tag{9}$$

where Q must be a positive definite real symmetrical matrix (or positive semi definite) with same dimension as matrix A, R must be a positive definite real symmetric matrix with order same as the column order of input matrix B. Those matrices Q and R are the optimal control coefficients that provide the expenditure of energy of the input signal. The control signal of Eq. (8) changes the state equation and performance index for regulation (*re* = 0), as in Eq. (10)-(12).

$$u(t) = -Kx(t) \tag{10}$$

$$\dot{x}(t) = (A - BK)x(t) \tag{11}$$

$$J = \int_0^\infty (x^T (Q + K^T RK) x dt \tag{12}$$

By letting a Hermitian positive definite function, P, Eq. (13) is established and can be simplified to satisfy any given states expressed in Ricatti equation form in Eq. (14).

$$x^T (Q + K^T RK)x = -\frac{d}{dt}(x^T Px) \tag{13}$$

$$A^T P + PA - PBR^{-1}B^T P + Q = 0 \tag{14}$$

For this control system to be stable, there must be one value of matrix P as positive definite to satisfy the above equation and for the regulator design, the states tend to zero as time approaches infinity. Thus, after simplifying the equation Eq. (14), the reduced Ricatti equation gives the control K as in Eq. (15).

$$K = R^{-1}B^T P \tag{15}$$

Thus, the design of LQR depends on the selection of Q and R since B is a constant quantity. In this study we have selected Q=[1 0 0 0 0 0 0 0;0 1 0 0 0 0 0 0;0 0 1 0 0 0 0 0;0 0 0 1 0 0 0 0;0 0 0 0 0.01 0 0 0;0 0 0 0 0 1 0 0;0 0 0 0 0 0 1000 0;0 0 0 0 0 0 0 1], and R=[.0002]. After solving for Eq. (14) for P and (15) for K, the optimal control gain was determined to be, K_o=[2760.6,155.6,-1819.6,-85.3,-416.0,66.2,-1308.4,-51.5]. These gains can be obtained using MATLAB command *lqr(A,B,Q,R)*.

B. Pole Placement Control (PPC)

To design PPC, the control gain K is obtained from the outlined design specifications i.e O_p and t_s. These specifications are then used to generate the dominant characteristics polynomial of the system. For the standard second order system, the general equation given in Eq. (16).

$$s^2 + 2\zeta\omega_n s + \omega_n^2 \tag{16}$$

It can be seen in Eq. (16) that, the natural frequency, ω and damping ratio, ζ of the system determine the dominant roots of the system. However, only two roots can be assigned from the second order equation using the outlined design specifications. Therefore, the remaining six poles can be assigned to be far away from the dominant poles. The solutions for ζ and ω are given in Eq. (17)-(18) in [17].

$$\zeta = \frac{\left|\ln\frac{1}{100}O_p\right|}{\sqrt{\left(\ln\frac{1}{100}O_p\right)^2 + \pi^2}} \tag{17}$$

$$\omega_n = \frac{4}{\zeta t_s} \tag{18}$$

Thus, the desired characteristics of the system derived from the selected Eigen values can be is as in Eq. (19).

$$(s-\mu_1)(s-\mu_2)...(s-\mu_n) = s^n + \varepsilon_{n-1}s^{n-1} + ...\varepsilon_1 s + \varepsilon_0 \tag{19}$$

where *n* is the order of the system, in this case eight. μ is the assigned Eigen value and ε is the coefficient of the polynomial terms. Likewise, the characteristics polynomial of the original system can be determine using Eq. (20).

$$|sI - A| = s^n + p_{n-1}s^{n-1} + p_{n-2}s^{n-2}...p_1 s + p_0 \tag{20}$$

where *p* is the coefficient of the polynomial term. Then, the state equation should be transformed to a controllable form using a transformation matrix M_T as in Eq. (21).

$$M_T = \begin{bmatrix} B & AB & ... & A^{n-1}B \end{bmatrix} \begin{bmatrix} p_1 & p_2 & ... & p_{n-1} & 1 \\ p_2 & p_3 & ... & 1 & \\ ... & ... & 1 & & \\ p_{n-1} & 1 & & & \\ 1 & & & & 0 \end{bmatrix} \tag{21}$$

Finally, the controller, K can be determined using Eq. (22.

$$K = \begin{bmatrix} \varepsilon_0 - p_0 & \varepsilon_1 - p_1 & ... & \varepsilon_{n-1} - p_{\varepsilon_{n-1} - p_{n-1}} \end{bmatrix} M_T^{-1} \tag{22}$$

After the necessary calculations, the selected Eigen values are: Poles = [-2±2.728i,-20±27.2875i,-26±35.4738i,-36.6± 49.92i] and the controller gain, K_p =10e4*[-2.7012,-0.0016,2.6191,-0.0031,0.0365,0.0042,-0.37 13,-0.0112]. Also, these gains can be obtained using MATLAB command *place(A,B,poles)*.

IV. DISCUSSION OF RESULTS

The parameters of Table 1 were used for the simulation analysis of the dynamic equations. The Simulink configuration for the MATLAB simulation is also illustrated in Fig. 4. It can be observed that the step input force serves as the actuator force for the sliding motion of the robot in the subsystem block. White noise and pulse signal served as the input disturbances while the control gains act as the feedback control. As stated earlier, only two outputs are considered for the analysis; robot base linear and angular displacements (y4 and β).

Initially, the response of the robot was studied with the initial condition of the states (without external excitation) for y4=0.2 and β=0.1. This describes the natural response of the robot. As stated by the Lyapunov theorem, stable and desired response should settle to zero as quickly as possible. As shown in Fig. 5 and Fig. 6, the response to initial condition without any control is vibratory and undesired. Thus, this confirmed the need to control the behavior of the system. In addition, LQR gives better response as compared to PPC.

Moreover, a step input force without external disturbance was analyzed. Fig. 7 shows the responses of the robot with and without control. Although both controllers demonstrated good control performance, LQR has better vibration suppression as compared to PPC. In addition, a pulse signal of magnitude 0.05 representing a sudden 50mm power line sagging is added to the system for 1 second. This serves as an uncertainty to the model. The responses are shown in Fig 8, and it shows that the PPC is highly affected by this external disturbance as compared to LQR. Also, a white noise random signal (noise power=0.5dB) is added to the system as a wind disturbance. This signal is expected to distort the motion of the robot and caused instability as shown in Fig. 9.

TABLE I. PARAMETERS FOR SIMULATION

λ1 = 0.12 m	λ2 = 0.13 m
m1 = m2 = 2.0 kg	M = 8.0 kg
k1 = k2 = 2.08E03 N/m	c1 = c2 = 10 Ns/m
k3 = k4 = 0.8E03 N/m	c3 = c4 = 30 Ns/m

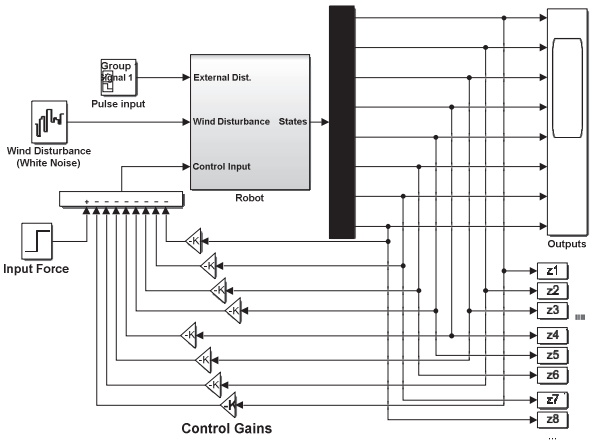

Fig. 4. Simulink Block for the Simulation.

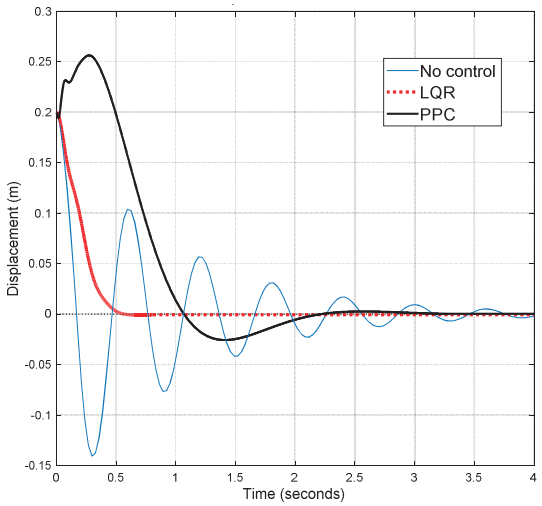

Fig. 5. Linear displacements to initial condition.

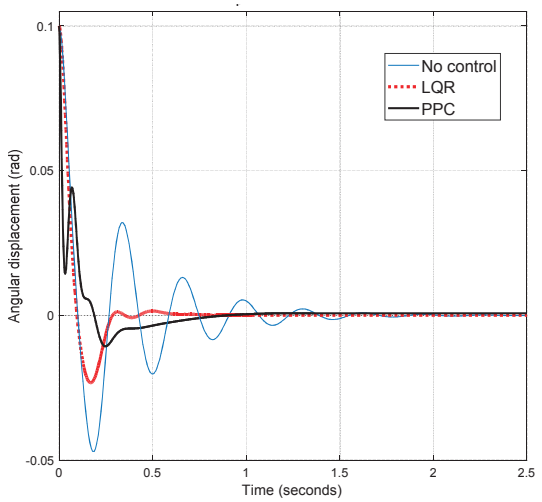

Fig. 6. Angular displacements for initial condition.

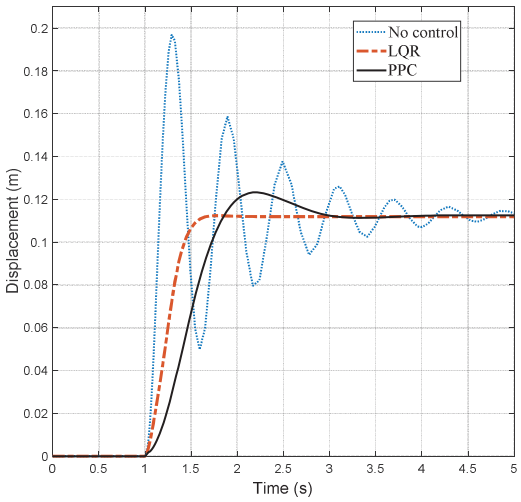

Fig. 7. Response to step input force.

Stability analysis of the system is presented in Fig. 10. It shows that the system is stable even without any control, however, the stability margin has been improved by the controllers.

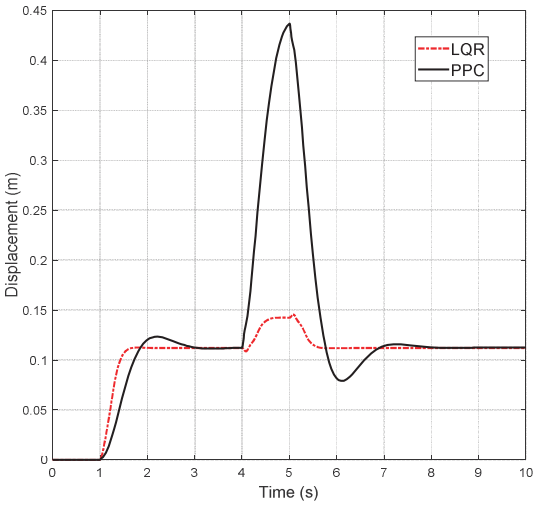

Fig. 8. Response to sudden power line sag disturbance.

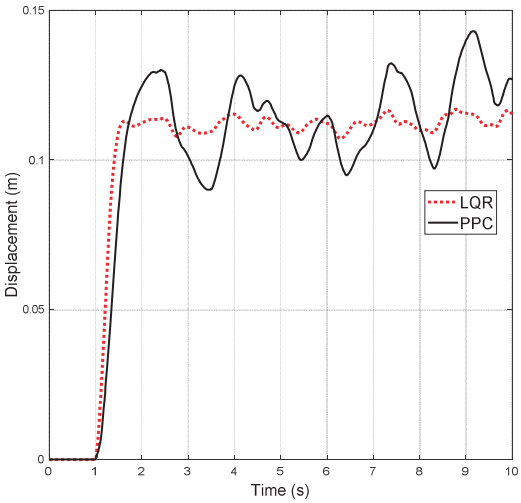

Fig. 9. Response to white noise as wind disturbance.

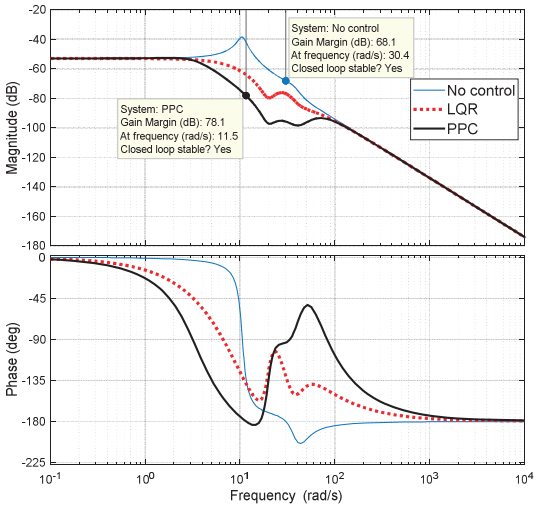

Fig. 10. Bode stability plot.

V. Conclusion

In conclusion, investigations into the modeling and optimal vibration control of a sliding of power transmission line

inspection robot modeled as a mass spring damper system have been presented. Lagrange's equation of motion was used for the derivation of the mathematical model. Natural and forced vibration responses were analyzed under the influence of initial condition and external excitation, respectively. Optimal linear quadratic regulator (LQR) controller was designed and its performance was compared to Pole placement control (PPC). MATLAB simulations result demonstrated that both controllers achieved the specified design specifications. However, LQR is more robust to uncertainties and external disturbance (wind) as compared to PPC. These results will be useful for an efficient and reliable inspection of power transmission lines.

ACKNOWLEDGMENT

The authors are grateful for the support provided by the Science and technology innovation project of Shaanxi province, China (No.2018ZDXM-GY-093).

REFERENCES

[1] J. Katra and F. Pernu, "A Survey of Mobile Robots for Distribution Power Line Inspection," *IEEE Trans. Power Deliv.*, vol. 25, no. 1, pp. 485–493, 2010.

[2] J. Guo, X. Zhang, H. Li, and X. Sun, "Mechanism Design and Strength Analysis of Key Components of Flight-climbing-slide Robot for High-voltage Transmission Line Inspection," in IEEE 7th Annual International Conference on Cyber Technology in Automation, Control and Intelligent System, pp. 200–205, August 2017.

[3] Zhao, G. Yang, E. Li, and Z. Liang, "Design and its visual servoing control of an inspection robot for power transmission lines," 2013 IEEE International Conference on Robotics and Biomimetics (ROBIO), pp. 546–551, 2013.

[4] D. Zhang, X. Zhang, and W. Jiang, "New power system for robots on transmission line," *Asia-Pacific Power Energy Eng. Conf. APPEEC*, pp. 4–7, 2010.

[5] M. Morita, H. Kinjo, and S. Sato, "Autonomous flight drone for infrastructure (transmission line) inspection (3)," *ICIIBMS 2017 - 2nd Int. Conf. Intell. Informatics Biomed. Sci.*, vol. 2018–January, no. 2, pp. 198–201, 2018.

[6] Y. Si, X. Li, H. Yu, Y. Li, Z. Yu, and J. Xu, "The flexible body dynamic analysis of the arms of automatic inspection robot for high-voltage transmission line," 2009 IEEE Int. Conf. Mechatronics Autom. ICMA 2009, no. 4, pp. 1737–1741, 2009.

[7] P. Debenest and M. Guarnieri, "Expliner - From prototype towards a practical robot for inspection of high-voltage lines," 2010 1st Int. Conf. Appl. Robot. Power Ind. CARPI 2010, pp. 1–6, 2010.

[8] P. Debenest, M. Guarnieri, K. Takita, E. F. Fukushima, S. Hirose, K. Tamura, A. Kimura, H. Kubokawa, N. Iwama, and F. Shiga, "Expliner - Robot for inspection of transmission lines," Proc. - IEEE Int. Conf. Robot. Autom., pp. 3978–3984, 2008.

[9] N. Pouliot, P. Latulippe, and S. Montambault, "Reliable and intuitive teleoperation of LineScout: A mobile robot for live transmission line maintenance," 2009 IEEE/RSJ Int. Conf. Intell. Robot. Syst. IROS 2009, pp. 1703–1710, 2009.

[10] S. Montambault and N. Pouliot, "Design and Validation of a Mobile Robot for Power Line," *Star*, pp. 495–504, 2008.

[11] J. Wang, A. Sun, C. Zheng, and J. Wang, "Research on a new crawler type inspection robot for power transmission lines," 2010 1st Int. Conf. Appl. Robot. Power Ind. CARPI 2010, pp. 1–5, 2010.

[12] J. Wang, X. Liu, K. Lu, Y. Liu, and J. Zhen, "A new bionic structure of inspection robot for high voltage transmission line," 2016 4th Int. Conf. Appl. Robot. Power Ind. CARPI 2016, pp. 1–4, 2016.

[13] W. T. Thomson, Theory of Vibrations with Applications, 5th ed. Santa Barbara, California: Chapman & Hall, 1998.

[14] A. B. Alhassan, X. Zhang, J. Guo, H. Shen, and H. Khaled, "Modelling, Simulation and Vibration Analysis of Transmission line Inspection Robot based on Mass Spring Damper Concept," in *International Conference on Applied Mathematics, Modeling and Simulation*, 2017, pp. 312–317.

[15] A. Alhassan, K. A. Danapalasingam, M. Shehu, A. M. Abdullahi, and A. Shehu, "Comparing the Performance of Sway Control Using ZV Input Shaper and LQR on Gantry Cranes," *Proc. - AMS 2015 Asia Model. Symp. 2015 - Asia 9th Int. Conf. Math. Model. Comput. Simul.*, pp. 61–66, 2016.

[16] Y. M. Sam, J. H. S. Osman, and M. R. A. Ghani, "A class of proportional-integral sliding mode control with application to active suspension system," Syst. Control Lett., vol. 51, no. 3–4, pp. 217–223, 2004.

[17] M. Shehu, M. R. Ahmad, A. Shehu, and A. Alhassan, "LQR, double-PID and pole placement stabilization and tracking control of single link inverted pendulum," Proc. - 5th IEEE Int. Conf. Control Syst. Comput. Eng. ICCSCE 2015, no. November, pp. 218–223, 2016.